Quantum spatial dynamics of high-gain parametric down-conversion accompanied by cascaded up-conversion

A. V. Rasputnyi* and D. A. Kopylov
Physics Department, Lomonosov Moscow State University, 119991 GSP-1, Leninskie Gory, Moscow, Russia

(Received 24 November 2020; accepted 21 June 2021; published 2 July 2021)

Quantum cascaded up-conversion (CUpC) of parametric down conversion (PDC) in a finite nonlinear $\chi^{(2)}$ crystal is studied theoretically within parametric approximation. The exact solution for creation and annihilation operators presented in the form of Bogoliubov transformation is valid for the high-gain regime and explicitly includes the nonzero wave-vector mismatch both for PDC and CUpC. Characteristic equation is used to analyze parametric amplification and oscillating regimes for degenerate, three- and four-mode cases. We show that the parametric amplification exists under the fulfillment of the cascaded phase-matching conditions while both the PDC and CUpC processes are separately non-phase-matched. The influence of CUpC on quadrature squeezing of degenerate PDC is estimated.

DOI: 10.1103/PhysRevA.104.013702

I. INTRODUCTION

Quantum light sources and frequency converters based on nonlinear optical effects are of special interest in quantum optics and technologies [1–3]. Nowadays, the most widespread nonclassical light sources are based on the second-order nonlinear effect of parametric down-conversion (PDC) [1]. PDC is the parametric amplification of electromagnetic vacuum fluctuations that occur in nonlinear crystals and lead to photon pair creation in so-called signal and idler modes. On the output of the crystal, the squeezed vacuum state [4] (or the bright squeezed vacuum state in the high-gain regime [5]) is realized. Signal and idler photons reveal quantum correlations that allow one, e.g., to prepare entangled states [3,6] and overcome shot-noise limit [7,8].

Simultaneously with PDC, signal and idler photons can be involved in the same nonlinear crystal into additional nonlinear processes, called "cascaded" or "multistep" processes [9]. One of such processes is the cascaded up-conversion (CUpC) of signal (or idler) PDC photons, which generally leads to coupling of four modes: signal, idler, and their up-converted modes. The CUpC of PDC is known also as "cascaded hyperparametric scattering" [1] or "parametric amplification at low-frequency pump" [10], when the seed in signal (or idler) wave is present.

PDC with CUpC is of interest as nonclassical light source with unique properties. The first observations of CUpC from PDC were obtained in the 1970s for the three-mode interaction, when CUpC process took place for the signal PDC mode [11,12], and the nonclassical statistical properties of the generated light were studied theoretically [13–17]. Later, the tripartite entangled states based on the CUpC were implemented [18–21] and the properties of the CUpC from high-gain PDC were experimentally studied [22,23]. In addition to the three-mode case, the degenerate regime (where signal and idler modes are not distinguishable) [24,25] and four-mode generation (where both the signal and idler waves are up-converted) [26,27] were theoretically considered.

The effect of PDC with CUpC arises also in the quantum frequency converters (QFC) that are used for the detection of IR radiation at the single-photon level [28,29] or for the entanglement support between remote ions [30]. The non-phase-matched PDC is present in QFC as a fundamental noise that was demonstrated, e.g., in Refs. [31–34].

The common quantum description of PDC with CUpC is realized in terms of the temporal evolution [16,17,20,25–27,35], while the nonzero wave-vector mismatch for considered nonlinear processes is omitted or involved effectively into the coupling constants with the use of short-length crystal approximation. However, the properties of quantum light generated via nonlinear optical effects are determined by the spatial dynamics of interacting waves in nonlinear crystal, e.g., correct accounting of nonzero wave-vector mismatches is critical for the broadband multimode high-gain PDC [36,37].

In contrast to the temporal evolution, the dynamics of the quantized electromagnetic field inside nonlinear crystals can be described in terms of the spatial evolution [38,39]. This approach was successfully applied to the PDC generation (e.g., Refs. [39–42]), analysis of optical harmonics generation from multimode broadband PDC [43,44], and the investigation of the properties of quantum nonlinear couplers [24,45].

In this paper, we apply the formalism of the spatial evolution of the quantized light to the PDC accompanied by CUpC. The paper is organized as follows: In Sec. II, we consider the main aspects of the studied nonlinear optical processes and reduce the initial Heisenberg equations for annihilation operators to the ordinary differential system for the Bogoliubov functions that is solved analytically. In Sec. III, the degenerate PDC with CUpC is studied and the oscillating regime and parametric amplification are analyzed. In addition, the influence of CUpC on PDC squeezing properties is considered.

*andrey@shg.ru

In Sec. IV, our approach is applied to the three- and four-mode CUpC of PDC and the parametric amplification for cascaded phase-matching conditions is demonstrated.

II. THEORETICAL APPROACH

For the quantum description of PDC coupled with CUpC in the transparent one-dimensional finite nonlinear crystal, we use the formalism based on momentum operator of the electromagnetic field [38,39]. In Heisenberg representation, the light that propagates along the z axis inside the dispersive medium is presented in terms of discrete temporal modes, with the frequencies $\omega_m = 2\pi m/T$, where $m = 0, 1, 2\ldots$ and T is quantization time. The electric field operator (the polarization indexes are omitted) has the form

$$\hat{E}(z,t) = \sum_{\omega} \sqrt{\frac{\hbar\omega}{2\epsilon_0 c T n(\omega)}} \hat{f}(\omega,z) e^{-i\omega t} + \text{H.c.}, \quad (1)$$

where $\hat{f}(\omega,z)$ and $\hat{f}^\dagger(\omega,z)$ are annihilation and creation operators with the bosonic commutation relations

$$[\hat{f}(\omega,z), \hat{f}^\dagger(\omega',z)] = \delta_{\omega\omega'},$$
$$[\hat{f}(\omega,z), \hat{f}(\omega',z)] = [\hat{f}^\dagger(\omega,z), \hat{f}^\dagger(\omega',z)] = 0. \quad (2)$$

The annihilation operators satisfy the Heisenberg equation [39]

$$\frac{d\hat{f}(\omega,z)}{dz} = \frac{i}{\hbar}[\hat{f}(\omega,z), \hat{G}(z)], \quad (3)$$

where the momentum operator $\hat{G}(z)$ is the generator for spatial evolution.

In this paper, we assume that the state on the input of the nonlinear crystal is vacuum one, and thus the quantum-mechanical averaging $\langle\ldots\rangle$ is obtained over the vacuum state $|0\rangle$. The mean number of photons $\mathcal{N}_\omega(z)$ in the mode $\hat{f}(\omega,z)$ has the form

$$\mathcal{N}_\omega(z) \equiv \langle 0|\hat{f}^\dagger(\omega,z)\hat{f}(\omega,z)|0\rangle. \quad (4)$$

In addition to the mean number of photons, the squeezing properties of interacting modes are studied. For the arbitrary collective mode

$$\hat{F}(\delta,z) = \frac{\hat{f}(\omega_1,z) + e^{i\delta}\hat{f}(\omega_2,z)}{\sqrt{2}}, \quad (5)$$

the quadrature operator

$$\hat{X}_F(\theta,\delta,z) = \hat{F}(\delta,z)e^{i\theta} + \hat{F}^\dagger(\delta,z)e^{-i\theta}. \quad (6)$$

can be introduced. For $\theta = 0$ and $\theta = \pi/2$, this operator corresponds to the position $\hat{Q}_F$ and momentum $\hat{P}_F$ quadratures, respectively. The variance of the quadrature (6) has the form

$$[\Delta X_F(\theta,\delta,z)]^2 = \langle \hat{X}_F^2(\theta,\delta,z)\rangle - \langle \hat{X}_F(\theta,\delta,z)\rangle^2. \quad (7)$$

The quadrature variance (7) depends on two parameters (θ,δ) and its minimal value $(\Delta X_F^{\min})^2$ can be used as the characteristic of the squeezing properties. For the vacuum state, the minimal variance of quadrature $(\Delta X_{\text{vac}}^{\min})^2 = 1$ and does not depend on the angles (θ,δ). For the arbitrary quantum state, the minimal variance $(\Delta X^{\min})^2$ can be either larger (antisqueezed state) or lower (squeezed state) than the vacuum one [Fig. 1(a)].

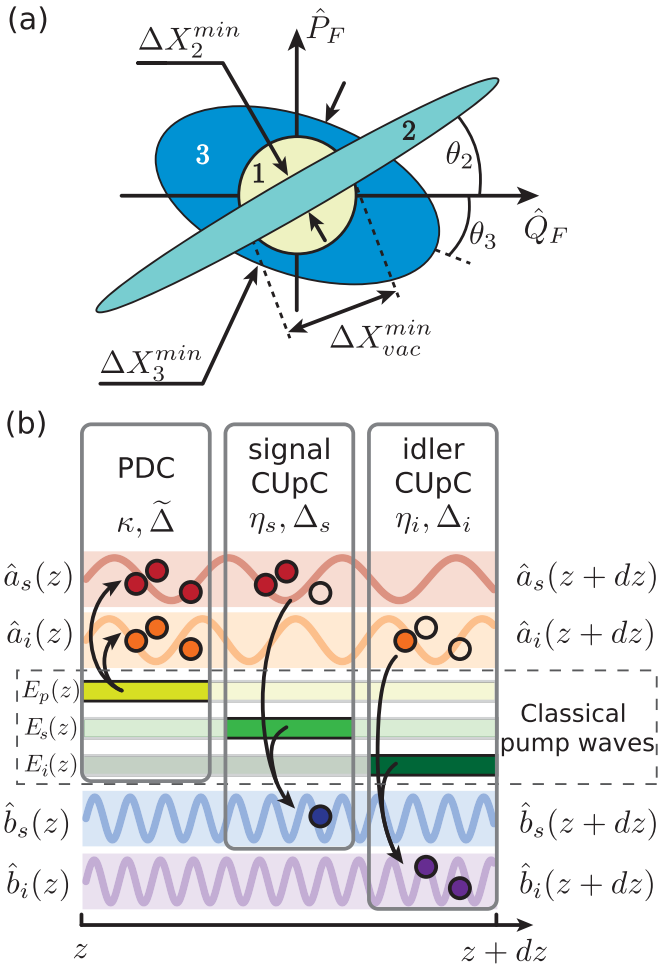

FIG. 1. (a) Phase space plot, showing the uncertainty for three different states: 1, vacuum state; 2, squeezed state with $(\Delta X_2^{\min})^2 < (\Delta X_{\text{vac}}^{\min})^2$; and 3, state with $(\Delta X_3^{\min})^2 > (\Delta X^{\min})^2$. The minimal quadrature variance for states 2 and 3 is achieved at angles θ_2 and θ_3, respectively. (b) Schematic representation of PDC with CUpC with multiple pump waves. At each point of the nonlinear crystal three simultaneous processes occur: PDC (photons are created in signal and idler modes) and cascaded up-conversion of signal photons and idler photons. In the case of a single pump wave, $E_p(z) \equiv E_i(z) \equiv E_s(z)$.

In the case of quadrature squeezing of single mode $\hat{f}(\omega,z)$, it is sufficient to consider the quadrature in the form $\hat{X}_f(\theta,z) = \hat{f}(\omega,z)e^{i\theta} + \hat{f}^\dagger(\omega,z)e^{-i\theta}$.

A. Spatial dynamics of PDC with CUpC

Our description of PDC with CUpC is based on several assumptions. First, we omit all the effects caused by the polarization of the light: The coupling of the interacting modes is described by effective susceptibilities. Second, the parametric approximation is applied: A classical monochromatic wave in the form $E_p = \frac{1}{2}\mathcal{E}_p e^{-i(\omega_p t - k_p z)} + \text{c.c.}$ is used as a pump wave, where $\mathcal{E}_p$ is the complex amplitude of the field, ω_p is pump frequency, and $k_p = k(\omega_p)$ is pump wave vector in the nonlinear crystal. The use of a monochromatic pump leads to the coupling between monochromatic PDC and CUpC modes and

instead of broadband radiation in the form (1) one can consider nonlinear interaction between separate monochromatic modes that satisfy the energy conservation law (the dynamic of broadband radiation can be assembled from the solution for monochromatic modes [39]).

As a result, three simultaneous second-order processes are considered in the nonlinear crystal: PDC ($\omega_p = \omega_{as} + \omega_{ai}$), signal CUpC ($\omega_p + \omega_{as} = \omega_{bs}$), and idler CUpC ($\omega_p + \omega_{ai} = \omega_{bi}$). Here and further in the text, the indexes a and b correspond to the PDC and CUpC modes, respectively, and indexes s and i indicate signal and idler waves. Thereby, four quantized modes are involved into the nonlinear interaction [Fig. 1(b)]:

$$\hat{a}_s(z) = \hat{\alpha}_s(z)e^{ik_{as}z} \equiv \hat{f}(\omega_{as}, z) \qquad \text{(PDC signal)}, \tag{8}$$

$$\hat{a}_i(z) = \hat{\alpha}_i(z)e^{ik_{ai}z} \equiv \hat{f}(\omega_{ai}, z) \qquad \text{(PDC idler)}, \tag{9}$$

$$\hat{b}_s(z) = \hat{\beta}_s(z)e^{ik_{bs}z} \equiv \hat{f}(\omega_{bs}, z) \qquad \text{(CUpC signal)}, \tag{10}$$

$$\hat{b}_i(z) = \hat{\beta}_i(z)e^{ik_{bi}z} \equiv \hat{f}(\omega_{bi}, z) \qquad \text{(CUpC idler)}, \tag{11}$$

where the slowly varying annihilation operators $\hat{\alpha}(z)$ and $\hat{\beta}(z)$ are introduced, and $k_n = k(\omega_n)$ are the wave vectors for each mode in nonlinear medium.

The momentum operator for studied system in Heisenberg representation consists of two terms $\hat{G}(z) = \hat{G}_l(z) + \hat{G}_{\text{nl}}(z)$. The linear part $\hat{G}_l(z)$ describes the propagation for each mode in the linear dielectric medium

$$\hat{G}_l(z) = \frac{\hbar}{2}\sum_{n=s,i}[k_{an}\hat{a}_n^\dagger(z)\hat{a}_n(z) + k_{bn}\hat{b}_n^\dagger(z)\hat{b}_n(z)] + \text{ H.c.} \tag{12}$$

The nonlinear term $\hat{G}_{\text{nl}}$ characterizes the nonlinear optical interaction that is present as a sum of two contributions, $\hat{G}_{\text{nl}}(z) = \hat{G}_{\text{pdc}}(z) + \hat{G}_{\text{upc}}(z)$, where

$$\hat{G}_{\text{pdc}}(z) = \hbar\kappa\ \hat{a}_s^\dagger(z)\hat{a}_i^\dagger(z)e^{ik_pz} + \text{H.c.} \tag{13}$$

corresponds to PDC (photon creation in signal and idler modes). The momentum operator for signal (s) and idler (i) CUpC is the following:

$$\hat{G}_{\text{upc}}(z) = \hbar\eta_s\ \hat{a}_s(z)\hat{b}_s^\dagger(z)e^{ik_pz} + \hbar\eta_i\ \hat{a}_i(z)\hat{b}_i^\dagger(z)e^{ik_pz} + \text{H.c.} \tag{14}$$

Here $\kappa \propto \chi^{(2)}_{\text{pdc}}\ \mathcal{E}_p$, $\eta_{s,i} \propto \chi^{(2)}_{s,i}\ \mathcal{E}_p$ are the complex coupling constants for PDC and for signal and idler CUpC, respectively. The $\chi_n^{(2)}$ are the effective nonlinear susceptibilities for each process.

By substituting (12), (13), and (14) into (3) and applying the expression $d\hat{a}(z)/dz = ik_a\hat{a}(z) + e^{ik_az}\ d\hat{\alpha}(z)/dz$, the two independent systems of Heisenberg equations for slowly varying operators are obtained. The first one is

$$\begin{cases} \frac{d\hat{\alpha}_s(z)}{dz} = i\kappa e^{i\widetilde{\Delta}z}\hat{\alpha}_i^\dagger(z) + i\eta_s^* e^{i\Delta_{s}z}\hat{\beta}_s(z), \\ \frac{d\hat{\beta}_s(z)}{dz} = i\eta_s e^{-i\Delta_{s}z}\hat{\alpha}_s(z), \\ \frac{d\hat{\alpha}_i^\dagger(z)}{dz} = -i\kappa^* e^{-i\widetilde{\Delta}z}\hat{\alpha}_s(z) - i\eta_i e^{-i\Delta_{i}z}\hat{\beta}_i^\dagger(z), \\ \frac{d\hat{\beta}_i^\dagger(z)}{dz} = -i\eta_i^* e^{i\Delta_{i}z}\hat{\alpha}_i^\dagger(z), \end{cases} \tag{15}$$

while the second one has the same form as (15) but with the replaced indexes $i \leftrightarrow s$. Here the $\widetilde{\Delta} = k_p - k_{as} - k_{ai}$ is the wave-vector mismatch of PDC and $\Delta_{s,i} = k_{bs,bi} - k_{as,ai} - k_p$ are the wave-vector mismatches of CUpC for signal (s) and idler (i) modes.

1. Multiple pump waves

One should notice that our approach and Eqs. (15) are valid also for the case when CUpC is generated by additional pump waves different from PDC pump. Then CUpC of each PDC mode can be initiated by its own monochromatic pump waves: $E_{s,i} = \frac{1}{2}\mathcal{E}_{s,i}e^{-i(\omega_{ps,pi}t - k_{ps,pi}z)} + \text{c.c.}$ [Fig. 1(b)]. Thus, the frequencies of signal CUpC and idler CUpC are $\omega_{bs,bi} = \omega_{ps,pi} + \omega_{as,ai}$, respectively, and each coupling parameter is proportional to the corresponding complex field amplitude: $\kappa \propto \mathcal{E}_p$, $\eta_{s,i} \propto \mathcal{E}_{s,i}$ with its own initial phase. In turn, the wave-vector mismatches $\Delta_{s,i} = k_{bs,bi} - k_{as,ai} - k_{ps,pi}$ can be independently controlled by varying pump frequencies.

Regardless of pump wave number and experimental realization (crystal type, pump lasers, etc.), the solution and analysis of PDC with CUpC can be performed in terms of six parameters: κ, η_s, η_i, $\widetilde{\Delta}$, Δ_s, Δ_i, and thus, further, without loss of generality we consider all this parameters independent.

2. Exact solution

In this paper, the exact solution of Eqs. (15) is found by using the approach presented in Ref. [36]. So far as the momentum operator has the bilinear form and the equations (15) are linear on creation and annihilation operators, the solution can be presented in the form of Bogoliubov transformation (see Appendix A)

$$\begin{pmatrix} \hat{\alpha}_s(z) \\ \hat{\beta}_s(z) \end{pmatrix} = \begin{pmatrix} U_s(z) & V_s(z) & W_s(z) & Q_s(z) \\ K_s(z) & L_s(z) & M_s(z) & N_s(z) \end{pmatrix} \begin{pmatrix} \hat{\alpha}_s(0) \\ \hat{\alpha}_i^\dagger(0) \\ \hat{\beta}_s(0) \\ \hat{\beta}_i^\dagger(0) \end{pmatrix}. \tag{16}$$

The similar transformation for the operators $\alpha_i(z)$ and $\beta_i(z)$ have the form (16) with replaced indexes $s \leftrightarrow i$.

By substituting (16) into the system (15) and combining the coefficients before the operators, one can get two differential systems for the introduced Bogoliubov's functions

$$\begin{cases} \frac{dU_s(z)}{dz} = i\kappa\ e^{i\widetilde{\Delta}z}\ V_i^*(z) + i\eta_s^*\ e^{i\Delta_{s}z}\ K_s(z), \\ \frac{dV_i^*(z)}{dz} = -i\kappa^* e^{-i\widetilde{\Delta}z}U_s(z) - i\eta_i e^{-i\Delta_{i}z}L_i^*(z), \\ \frac{dK_s(z)}{dz} = i\eta_s\ e^{-i\Delta_{s}z}\ U_s(z), \\ \frac{dL_i^*(z)}{dz} = -i\eta_i^*\ e^{i\Delta_{i}z}\ V_i^*(z), \\ U_s(0) = 1, V_i^*(0) = 0, K_s(0) = 0, L_i^*(0) = 0, \end{cases} \tag{17}$$

$$\begin{cases} \frac{dW_s(z)}{dz} = i\kappa e^{i\widetilde{\Delta}z}\ Q_i^*(z) + i\eta_s^*\ e^{i\Delta_{s}z}\ M_s(z), \\ \frac{dQ_i^*(z)}{dz} = -i\kappa^* e^{-i\widetilde{\Delta}z}W_s(z) - i\eta_i e^{-i\Delta_{i}z}N_i^*(z), \\ \frac{dM_s(z)}{dz} = i\eta_s\ e^{-i\Delta_{s}z}\ W_s(z), \\ \frac{dN_i^*(z)}{dz} = -i\eta_i^*\ e^{i\Delta_{i}z}\ Q_i^*(z), \\ W_s(0) = 0, Q_i^*(0) = 0, M_s(0) = 1, N_i^*(0) = 0. \end{cases} \tag{18}$$

The equations for the functions $U_i(z)$, $V_s^*(z)$, $K_i(z)$, $L_s^*(z)$, and $W_s(z)$, $Q_i^*(z)$, $M_s(z)$, $N_i^*(z)$ are similar to Eqs. (17) and (18), respectively, but with replaced indexes $i \leftrightarrow s$.

Thus, the initial systems of differential equations for the operators (15) are transformed to the systems of ordinary differential equations for Bogoliubov functions (16). This system can be solved by the standard methods of differential equations, including numerical ones. After the Bogoliubov functions are calculated, all the averaged values of the field on the output of the crystal for a given input state can be calculated, including number of photons (4) and quadrature variance (7).

It should be noted that Bogoliubov transformation (16) is valid for any coupling constants and wave-vector mismatches and determines the exact solution of studied system (15) that gives a possibility to study the high-gain regime of PDC accompanied by CUpC.

3. Averaged solution

The alternative way to study the CUpC of PDC with nonzero wave-vector mismatch is to exploit averaging over the crystal length L (this approach can be found, e.g., in Refs. [25,40]). Applying this procedure to the oscillating terms $e^{i\Delta z}$, one can obtain

$$\zeta(\Delta) = \frac{1}{L}\int_0^L dz\, e^{i\Delta z} = \mathrm{sinc}\left(\frac{\Delta L}{2}\right) e^{\frac{i\Delta L}{2}}, \tag{19}$$

and in the system (15) the wave-vector mismatch is effectively considered by multiplying the initial coupling parameters on the averaged values: $\kappa \to \kappa \times \zeta(\widetilde{\Delta})$, $\eta_i \to \eta_i \times \zeta(\Delta_i)$, and $\eta_s \to \eta_s \times \zeta(\Delta_s)$.

So the initial system with nonzero wave-vector mismatch is replaced by the phase-matched system with reduced coupling constants. After averaging, Eqs. (15) become autonomous and their solutions were obtained for different cases of PDC with CUpC in Refs. [16,20,25–27,35]. For the initial nonautonomous system of Eqs. (15), this solution is approximate and differs from the exact one, presented in terms of Bogoliubov transformations (16).

B. Characteristic equation

For the system of differential equations (17) and (18), the analytical solution is found (see Appendix B). In spite of this, its direct analysis is sophisticated: There are 16 complex Bogoliubov functions which depend on three complex parameters κ, η_s, η_i and three real ones $\widetilde{\Delta}$, Δ_s, Δ_i. However, from the analytical solution for Bogoliubov functions (B8), (B9), one can notice that Bogoliubov functions reveal exponential spatial dependence (see Appendix B)

$$U(z), V(z)... \sim e^{\lambda z}. \tag{20}$$

Here λ are the roots of characteristic equation that has the depressed quartic form (see Appendix B 3)

$$\lambda^4 + P\lambda^2 + iQ\lambda + R = 0, \tag{21}$$

where

$$P = g_s^2 + g_i^2 + \frac{\phi^2}{2} - |\kappa|^2, \tag{22}$$

$$Q = \phi(g_i^2 - g_s^2) - |\kappa|^2 \frac{\Delta_i - \Delta_s}{2}, \tag{23}$$

$$R = \left[g_s^2 - \frac{\phi^2}{4}\right]\left[g_i^2 - \frac{\phi^2}{4}\right] - \frac{|\kappa|^2}{4}(\phi - \Delta_s)(\phi - \Delta_i), \tag{24}$$

and $g_s^2 = |\eta_s|^2 + \Delta_s^2/4$, $g_i^2 = |\eta_i|^2 + \Delta_i^2/4$, and $\phi = \widetilde{\Delta} - (\Delta_s + \Delta_i)/2$.

So far as the roots of characteristic equation (21) are complex, their imaginary parts lead to the oscillating terms in Bogoliubov functions, while the positive real parts lead to the exponentially increasing contributions. Thus, the parametric amplification exists when at least one of the roots of the characteristic equation has a real positive part. At some distance the exponentially increasing terms predominate over the oscillating contributions and the high-gain regime of PDC with CUpC can be realized (in this case, the mean number of photons is larger than 1).

In a general case, while all the parameters κ, η_s, η_i, $\widetilde{\Delta}$, Δ_s, Δ_i are independent, the roots of the characteristic equation take sophisticated form. Nevertheless, the nature of the roots defines the criteria for parametric amplification and the quartic equation can be obtained from the set of inequalities that involves the discriminant and the parameters P, Q, R (see Appendix B 3 and Ref. [46]).

C. Experimental ranges of coupling constants

Let us discuss the experimental parameters when PDC with CUpC could be realized. In the case of a single pump wave, the wave-vector mismatches are fixed and determined by the dispersion of nonlinear crystals. The coupling parameters $|\kappa|$ and $|\eta_{s,i}|$ linearly depend on the pump amplitude, while the ratios $r_{s,i} = |\eta_{s,i}|/|\kappa|$ are determined by the crystal parameters (refractive indexes and effective nonlinear susceptibilities), e.g., for degenerate PDC from BBO crystal pumped by 800 nm $r \approx 0.9$. As a result, the coupling parameters could be assumed to be on the same order $|\eta_{s,i}| \sim |\kappa|$. The typical experimental gain value for the phase-matched high-gain PDC is ≈5–10 [5], and for the crystal length $L = 0.5$–2 cm the PDC coupling takes the values of $\kappa \approx 1$–20 cm^{-1} (to the best of our knowledge, the maximal experimental coupling constant $\kappa \approx 36$ cm^{-1} was achieved in Ref. [23]).

The most flexible and controllable way to obtain PDC with CUpC is to use multiple pump lasers, when each coupling constant is proportional to the corresponding pump amplitude. Consequently, each coupling parameter could be varied independently (e.g., in Ref. [21] experimental coupling constants are κ, $\eta_s \approx 3$–6 cm^{-1}).

In order to consider the main aspects of PDC with CUpC, we do not focus on the specific experimental realization of studied processes; however, we use the values achievable in experiments. So, for the analysis, we take $\kappa = 3$ cm^{-1} and $L = 2$ cm (parametric gain $\Gamma = 6$) and consider PDC with CUpC close to the phase matching. Using these parameters, the main features of high-gain PDC accompanied by CUpC are demonstrated further, in Secs. III and IV.

Summarizing Sec. II, the exact solution of PDC with CUpC is presented in terms of Bogoliubov transformation and all the observable values of electromagnetic field and their spatial

dynamics along the nonlinear crystal can be expressed in terms of Bogoliubov functions. The root analyses of characteristic equation provide the criterion for the parametric amplification and in the next sections are explicitly presented for degenerate and three- and four-mode cases of PDC with CUpC.

III. RESULTS AND DISCUSSION: DEGENERATE CASE

Let us consider frequency degenerate case when the two interacting modes are present: the degenerate PDC mode with the wave vector k_a and the frequency $\omega_a = \omega_p/2$; and the CUpC mode with the wave vector k_b and the frequency $\omega_b = \omega_p/2 + \omega_{ps}$ (for the single pump scheme $\omega_b = 3\omega_p/2$). In this case $\eta_i = \eta_s$ and $\Delta_i = \Delta_s$ and all the indexes i and s in the Bogoliubov transformation (16) can be omitted.

The number of photons in PDC and CUpC modes are

$$\mathcal{N}_a(z) \equiv \langle 0|\hat{a}^\dagger(z)\hat{a}(z)|0\rangle = |V(z)|^2 + |Q(z)|^2, \tag{25}$$

$$\mathcal{N}_b(z) \equiv \langle 0|\hat{b}^\dagger(z)\hat{b}(z)|0\rangle = |L(z)|^2 + |N(z)|^2. \tag{26}$$

The quadrature variances for PDC $[\Delta X_a(\theta_a, z)]^2$ and CUpC $[\Delta X_b(\theta_b, z)]^2$ have the form

$$[\Delta X_j(\theta_j, z)]^2 = 1 + 2\mathcal{N}_j(z) + 2|F_j(z)|\cos(2\theta_j + \varphi_j), \tag{27}$$

where index $j = a, b$ corresponds to the PDC and CUpC modes, respectively. Here correlation functions $F_a(z) \equiv \langle \hat{a}(z)\hat{a}(z)\rangle$ and $F_b(z) \equiv \langle \hat{b}(z)\hat{b}(z)\rangle$ are

$$F_a(z) = \big[U(z)V(z) + W(z)Q(z)\big]e^{i2k_a z}, \tag{28}$$

$$F_b(z) = \big[K(z)L(z) + M(z)N(z)\big]e^{i2k_b z} \tag{29}$$

and $\varphi_j = \arg[F_j(z)]$. As stems from (27), the minimal quadrature variances $(\Delta X_a^{\min})^2$ and $(\Delta X_b^{\min})^2$ are obtained for the angles $\theta_a = (\pi - \varphi_a)/2$ and $\theta_b = (\pi - \varphi_b)/2$, respectively.

In addition, the two-mode squeezing for the collective PDC-CUpC operator can be presented as

$$\hat{C}(\delta) = \frac{\hat{a}(z) + e^{i\delta}\hat{b}(z)}{\sqrt{2}}, \tag{30}$$

where δ is the arbitrary phase. Its quadrature variance has the form

$$[\Delta X_C(\theta, \delta, z)]^2 = \frac{[\Delta X_a(\theta, z)]^2 + [\Delta X_b(\theta + \delta, z)]^2}{2} + 2|F_{ab}(z)e^{i2\theta} + G_{ab}(z)|\cos[\delta + \phi(z)], \tag{31}$$

where correlation functions $F_{ab}(z) \equiv \langle \hat{a}(z)\hat{b}(z)\rangle$ and $G_{ab}(z) \equiv \langle \hat{a}^\dagger(z)\hat{b}(z)\rangle$ have the form

$$F_{ab}(z) = \big[U(z)L(z) + W(z)N(z)\big]e^{i(k_a+k_b)z}, \tag{32}$$

$$G_{ab}(z) = \big[V^*(z)L(z) + Q^*(z)N(z)\big]e^{-i(k_a-k_b)z}, \tag{33}$$

$$\phi(z) = \arg\big[F_{ab}(z)e^{i2\theta} + G_{ab}(z)\big]. \tag{34}$$

The minimal value of the variance $[\Delta X_C^{\min}(z)]^2 = [\Delta X_C(\theta_{\min}, \delta_{\min}, z)]^2$ does not have a simple analytical form and should be solved numerically.

A. PDC without CUpC

Before the CUpC properties are considered, we examine our approach for the PDC generation in the absence of CUpC. In this case, we assume that the coupling constants $\eta_s = \eta_i \to 0$, and the roots of the characteristic equation (21) have the form

$$\lambda_{1,2} = \pm\gamma, \ \lambda_{3,4} = \pm i\widetilde{\Delta}/2, \tag{35}$$

where $\gamma = \sqrt{|\kappa|^2 - \widetilde{\Delta}^2/4}$.

By substituting the roots (35) into the solution (B8) and (B9) with the parameters $\eta_s = \eta_i \to 0$, $\Delta_s = \Delta_i \to 0$, one obtains the nonzero Bogoliubov functions

$$U(z) = \left[\cosh(\gamma z) - \frac{i\widetilde{\Delta}}{2\gamma}\sinh(\gamma z)\right]e^{i\widetilde{\Delta}z/2}, \tag{36}$$

$$V(z) = \frac{i\kappa}{\gamma}\sinh(\gamma z)e^{i\widetilde{\Delta}z/2}, \tag{37}$$

that correspond to the well-known solution for the PDC generation, e.g., Refs. [1,39,47].

On the output of the crystal with the length L the number of photons for PDC mode has the form

$$\mathcal{N}_a(L) = |V(L)|^2 = |\kappa|^2 L^2\left[\frac{\sinh(\Gamma)}{\Gamma}\right]^2. \tag{38}$$

The dimensionless parameter $\Gamma = \gamma L$ is known as the parametric gain for PDC process [1,5]. In the case of $\Gamma \gtrsim 1$ the high-gain regime is realized: mean number of photons $\mathcal{N}_a \gg 1$.

One can see that two roots $\lambda_{1,2}$ are real if $|\kappa| > |\widetilde{\Delta}|/2$ [Eq. (35)] and according Eq. (38) the number of photons increases exponentially, i.e., the parametric amplification occurs. Otherwise, all the roots of characteristic equation are imaginary and Bogoliubov functions (37) are oscillating. Thus, our statement about determination of parametric amplification by the nature of the roots of characteristic equation (Subsec. II B) is valid for PDC generation.

For the phase-matched PDC ($\widetilde{\Delta} = 0$), the minimal variance of the quadrature operator $\hat{X}_a(\theta, z) = \hat{a}(z)e^{i\theta} + \hat{a}^\dagger(z)e^{-i\theta}$ has the form

$$(\Delta X_a^{\min})^2 = 1 + 2\mathcal{N}_a - 2|UV| = e^{-2\Gamma}. \tag{39}$$

So far as the up-conversion process is absent, the CUpC mode remains a vacuum.

B. Degenerate PDC with CUpC: Characteristic equation and roots analysis

In this subsection, we apply our approach to the analysis of the degenerate PDC with CUpC. The characteristic equation (21) becomes biquadratic ($Q = 0$) with the coefficients

$$P = 2|\eta_s|^2 + \Delta_s^2 + \frac{\widetilde{\Delta}(\widetilde{\Delta} - 2\Delta_s)}{2} - |\kappa|^2, \tag{40}$$

$$R = \left[|\eta_s|^2 - \frac{\widetilde{\Delta}(\widetilde{\Delta} - 2\Delta_s)}{4}\right]^2 - \frac{|\kappa|^2}{4}(\widetilde{\Delta} - 2\Delta_s)^2 \tag{41}$$

TABLE I. Conditions for different cases of roots of characteristic equation for the degenerate CUpC of PDC. $\mathbb{R}$ is real number, $\mathbb{I}$ is imaginary number, and $\mathbb{C}$ is complex with nonzero real and imaginary parts.

Area	Condition	Roots
I	$P > 0$ and $0 < R < P^2/4$	$\lambda_{1,2,3,4} \in \mathbb{I}$
II	$R < 0$	$\lambda_{1,2} \in \mathbb{R}$, $\lambda_{3,4} \in \mathbb{I}$
III	$R > P^2/4$	$\lambda_{1,2,3,4} \in \mathbb{C}$
IV	$P < 0$ and $0 < R < P^2/4$	$\lambda_{1,2,3,4} \in \mathbb{R}$
V	$R = P^2/4$ or $R = 0$	Multiple roots

and the roots are easily obtained:

$$\lambda_{1,2,3,4} = \pm\sqrt{\frac{-P \pm \sqrt{P^2 - 4R}}{2}}. \tag{42}$$

There are five possible cases of roots which define the behavior of solution (Table I). The description of these cases is accompanied by the diagrams $\Delta_s - \eta_s$ in Figs. 2 and 3. Figures 2(a) and 3(a) demonstrate the phase diagrams where different colors represent different regimes of generation. In addition, the number of photons and the minimal variance of quadratures for high-gain regime are also presented in Figs. 2 and 3 (details are in the captions). For completeness, the spatial dynamics of photon number and minimal quadrature variance for the PDC and CUpC modes are plotted in Fig. 4.

The numerical analysis is provided for $\kappa = 3$ cm^{-1} and the crystal length $L = 2$ cm both for the phase-matched PDC ($\widetilde{\Delta} = 0$, Fig. 2) and for the non-phase-matched PDC ($\widetilde{\Delta} = 10$ cm^{-1}, Fig. 3).

1. Area I

All the roots $\lambda_{1,2,3,4}$ are imaginary and $\lambda_{3,4} = \lambda_{1,2}^*$. Generally, this is the single regime which corresponds to the absence of the parametric amplification and leads to quasiperiodic solution for Bogoliubov functions. According to Figs. 2(b), 2(c), 3(b), and 3(c), inequality $\mathcal{N}_{a,b} < 1$ is valid both for PDC and CUpC modes.

2. Area II

In this case, two roots are real and thus the parametric amplification occurs. From Figs. 2(b), 2(c), 3(b), and 3(c), one can see that the number of CUpC photons is at least one order of magnitude lower compared to the number of PDC photons. Increasing the parameter Δ_s for the phase-matched PDC generation [Figs. 2(b) and 2(c)] leads to decrease of the CUpC efficiency and in this regime the CUpC can be considered as loss for the PDC radiation. In detail, this case is considered below in Subsec. III C.

From Fig. 4(a), one can see that the number of photons both for PDC and CUpC modes increases exponentially all over the nonlinear crystal. However, the CUpC mode remains unsqueezed, and the squeezing of the PDC mode is limited and reaches the constant value during the propagation (for details, see Subsec. III C).

For the non-phase-matched PDC generation area II still exists [Figs. 3(b) and 3(c)] and parametric amplification for both modes with nonzero wave-vector mismatch can be achieved.

3. Area III

In this regime, all the roots are complex numbers with the nonzero real and imaginary parts. The parametric amplification inside the crystal is accompanied by the periodic energy

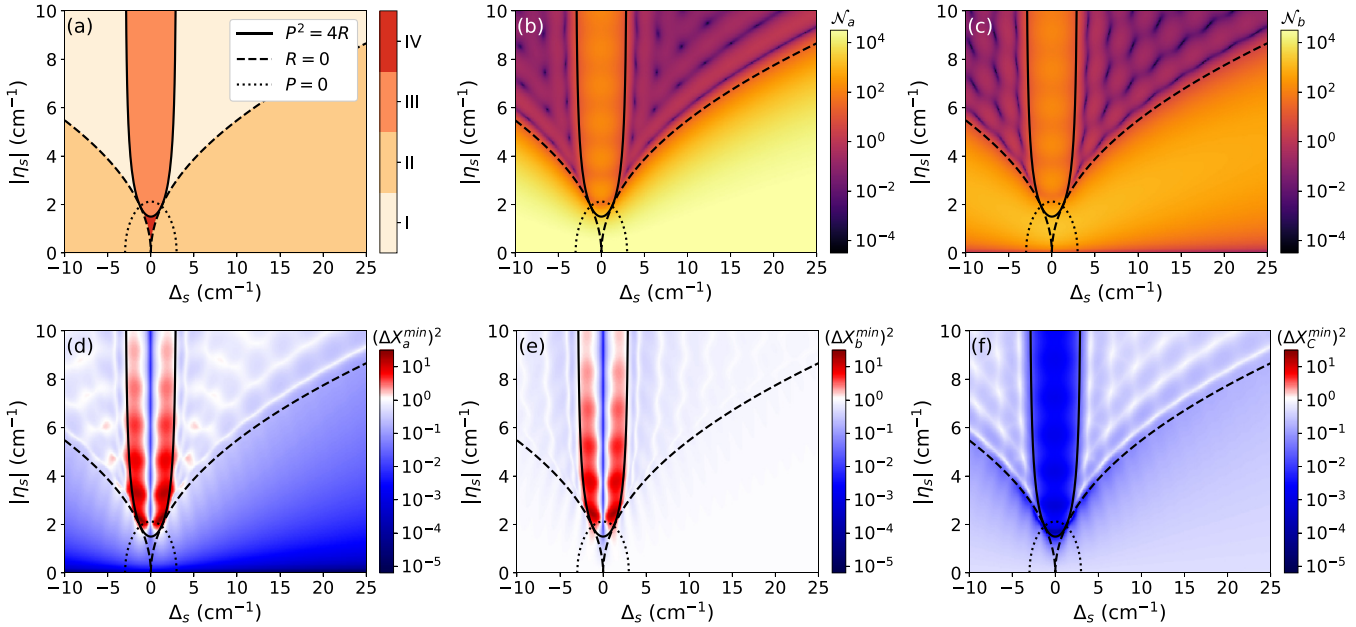

FIG. 2. Diagrams $\Delta_s - \eta_s$ for degenerate CUpC of PDC, for the phase-matched PDC case ($\widetilde{\Delta} = 0$, $|\kappa| = 3$ cm^{-1}): (a) the phase diagram (different colors correspond to different regimes of generation); [(b), (c)] number of photons $\mathcal{N}_a$ (PDC mode) and $\mathcal{N}_b$ (CUpC mode), respectively; [(d)–(f)] minimal quadrature variances $(\Delta X_a^{\min})^2$ (PDC mode), $(\Delta X_b^{\min})^2$ (CUpC mode), and $(\Delta X_C^{\min})^2$ (collective PDC-CUpC), respectively. Number of photons and minimal quadrature variances are calculated for the crystal length $L = 2$ cm.

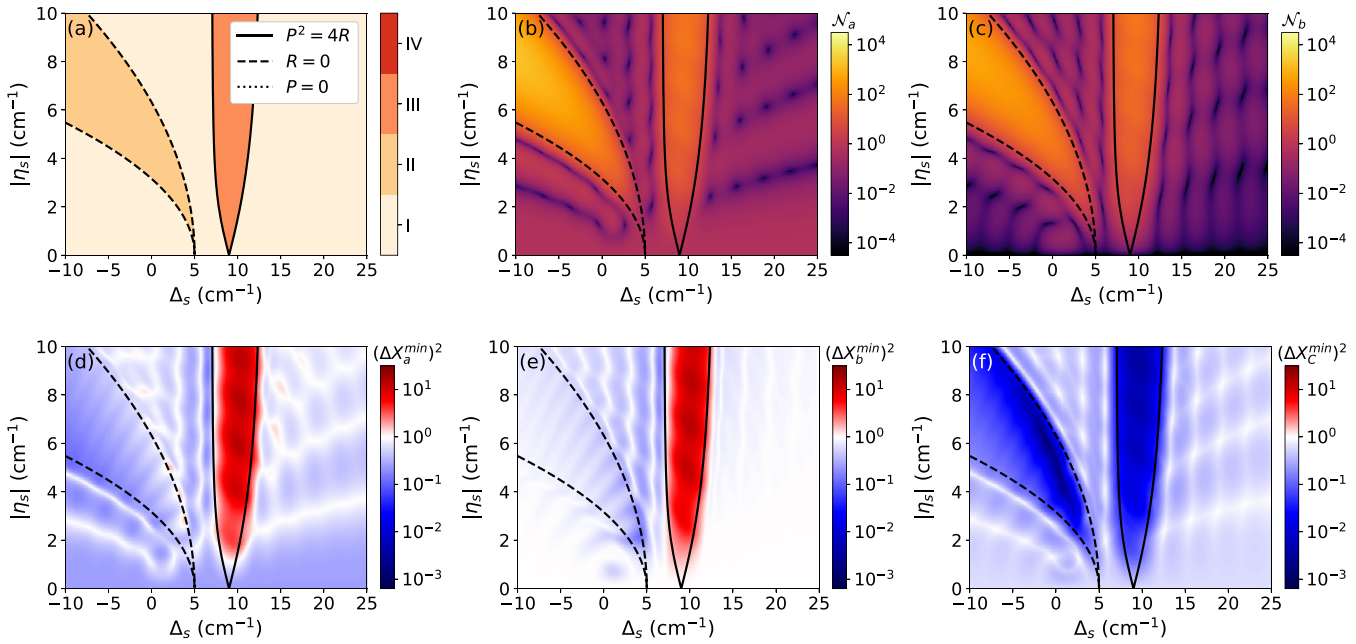

FIG. 3. Diagrams $\Delta_s - \eta_s$ for degenerate CUpC of PDC, for the non-phase-matched PDC case ($\widetilde{\Delta} = 10$ cm^{-1}, $|\kappa| = 3$ cm^{-1}): (a) the phase diagram (different colors correspond to different regimes of generation); [(b), (c)] number of photons $\mathcal{N}_a$ (PDC mode) and $\mathcal{N}_b$ (CUpC mode), respectively; [(d)–(f)] minimal quadrature variances $(\Delta X_a^{\min})^2$ (PDC mode), $(\Delta X_b^{\min})^2$ (CUpC mode), and $(\Delta X_C^{\min})^2$ (collective PDC-CUpC), respectively. Number of photons and minimal quadrature variances are calculated for crystal length $L = 2$ cm.

transfer between PDC and CUpC modes [Figs. 4(c) and 4(d)] and $\mathcal{N}_a \approx \mathcal{N}_b$ in the whole area III [Figs. 2(b), 2(c) 3(b), and 3(c)].

If both processes are phase matched ($\widetilde{\Delta} = 0$, $\Delta_s = 0$), the PDC and CUpC modes are simultaneously squeezed [Figs. 2(d) and 2(e)] $(\Delta X_a^{\min})^2 \approx (\Delta X_b^{\min})^2$. However, a small variation of Δ_s leads to dramatic change of the single-mode squeezing properties of generated light. Considering spatial evolution of the minimal single-mode quadrature variances, we see that it starts to increase at some point both for PDC and CUpC radiation, which is shown in Fig. 4(d). The qualitative analysis of this effect shows that PDC and CUpC modes possess separate quadrature squeezing when $\theta_a = \theta_b + \pi/2$.

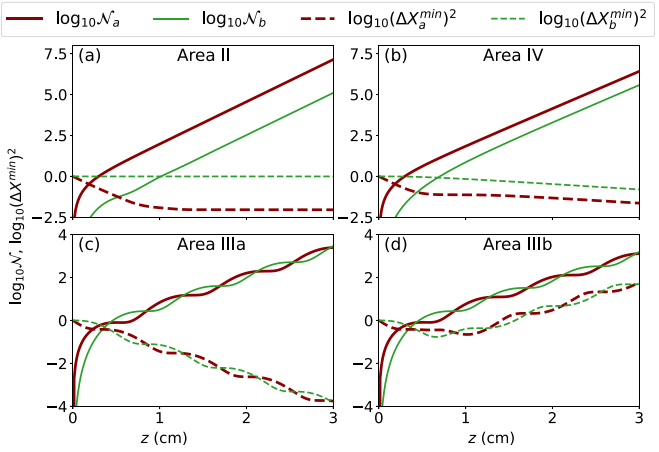

FIG. 4. The dependence of number of photons and minimal quadrature variances for PDC and CUpC modes on the nonlinear crystal length for the phase-matched PDC case ($\widetilde{\Delta} = 0$, $|\kappa| = 3$ cm^{-1}): (a) area II ($\Delta_s = 10$ cm^{-1}, $\eta_s = 1$ cm^{-1}), (b) area IV ($\Delta_s = 0$ cm^{-1}, $\eta_s = 1$ cm^{-1}), (c) area III ($\Delta_s = 0$ cm^{-1}, $\eta_s = 4$ cm^{-1}), and (d) area III ($\Delta_s = 0.5$ cm^{-1}, $\eta_s = 4$ cm^{-1}).

Out of the phase-matched PDC ($\widetilde{\Delta} = 0$), both the PDC and CUpC modes are antisqueezed in area III [Figs. 3(d) and 3(e)]. However, the two-mode (PDC-CUpC) squeezing for the collective operator $\hat{C}$ [Eq. (5)] is always achieved [Figs. 2(f) and 3(f)].

4. Area IV

Here all the roots $\lambda_{1,2,3,4}$ are real. As we see in Figs. 4(a) and 4(b), this regime is similar to area II and the most effective generation of CUpC can be obtained.

5. Area V: Multiple roots

If coupling constants and phase mismatches satisfy conditions $R = 0$ or $R = P^2/4$, the roots of the characteristic equation are multiple, and, strictly speaking, the analytical solution in the form presented in Appendix B is not valid. Nevertheless, according to the initial equation (B1) the solution does not have any singularities and discontinuities in the case of multiple roots and the expressions (B8) and (B9) can be used in limiting case, taking parameters as close to the curves $R = 0$ or $R = P^2/4$ as possible. The detailed analysis of multiple roots is not considered in this paper.

6. Phase-matched PDC with CUpC ($\Delta_s = 0$, $\widetilde{\Delta} = 0$)

A simple form of roots can be obtained for degenerate phase-matched PDC with CUpC ($\Delta_s = 0$, $\widetilde{\Delta} = 0$):

$$\lambda_{1,2,3,4} = \pm\frac{|\kappa|}{2} \pm \sqrt{|\kappa|^2/4 - |\eta_s|^2}. \tag{43}$$

If $|\kappa|^2/4 > |\eta_s|^2$, all the roots are real and this corresponds to area IV. When $|\kappa|^2/4 < |\eta_s|^2$, the real part of roots λ_i is equal to the $\pm|\kappa|/2$ and is independed on parameter η_s. Hence, in area III we observe some kind of oscillating plateau in Figs. 2(b) and 2(c) for photon numbers and in Figs. 2(d)–2(f) for one- and two-mode squeezing. So far as the real part of characteristic equation roots are responsible for the parametric amplification, in the high-gain regime $\mathcal{N}_a \approx \mathcal{N}_b \approx \sinh^2(\widetilde{\Gamma})$, where $\widetilde{\Gamma} = |\kappa|L/2$ is the half from phase-matched PDC generation with the absence of CUpC.

C. Particular case: Strongly phase-mismatched CUpC as losses for degenerate PDC

In this subsection, we consider one of the important practical cases appearing with a single pump wave: phase-matched PDC ($\widetilde{\Delta} = 0$) with large CUpC wave-vector mismatch ($\Delta_s \gg |\kappa|, |\eta_s|$). For this reason, we introduce small parameters $\epsilon_a = |\kappa|/\Delta_s \ll 1$ and $\epsilon_b = |\eta_s|/\Delta_s \ll 1$ and obtain approximation of general solution for this special case. The roots of characteristic equation satisfy conditions for area II:

$$\lambda_{1,2} \approx \pm|\kappa|(1-\epsilon_b^2), \quad \lambda_{3,4} \approx \pm i\Delta_s(1+\epsilon_b^2). \tag{44}$$

Considering exact solution (B9), an approximate number of photons is obtained, keeping the first nonvanishing term with ϵ_b^2:

$$\mathcal{N}_a \approx (1-\epsilon_b^2)\sinh^2\tilde{\Gamma}, \tag{45}$$

$$\mathcal{N}_b \approx \epsilon_b^2 \sinh^2\tilde{\Gamma}, \tag{46}$$

where $\tilde{\Gamma} = |\kappa|L(1-\epsilon_b^2)$. In this case, the CUpC is inefficient compared to PDC and can be assumed as losses for PDC mode.

As the squeezing properties are sensitive to the losses, we obtain minimal variance of quadrature for the PDC mode:

$$(\Delta X_a^{\min})^2 \approx (1-\epsilon_b^2)e^{-2\tilde{\Gamma}} + \epsilon_b^2. \tag{47}$$

As mentioned above (see Subsec. II C), the coupling constants $|\kappa|$ and $|\eta_s|$ linearly depend on the pump amplitude, while the ratio $r = |\eta_s|/|\kappa|$ is determined by the crystal parameters. Thus, the PDC squeezing (47) as a function of pump power becomes more complicated compared to the PDC generation (39)

$$(\Delta X_a^{\min})^2 \approx (1-\delta^2\Gamma^2)e^{-2\Gamma(1-\delta^2\Gamma^2)} + \delta^2\Gamma^2, \tag{48}$$

where $\delta = r(\Delta_s L)^{-1}$ is small and $\Gamma = |\kappa|L$ is a dimensionless parameter that corresponds to parametric gain of PDC without CUpC (38).

In Figs. 5(a) and 5(b), the number of photons for PDC and CUpC modes and the minimal variance for the PDC mode $(\Delta X_a^{\min})^2$, respectively, are shown as functions of parameter Γ. The calculation is provided with $\Delta_s L = 15\pi$ and $r = 1$ for two models: the exact one [Eqs. (17) and (18)] and the averaged one obtained using Eq. (19). One can see that the number of photons, calculated by both models, does not significantly differ from each other and for PDC are of the same order as without CUpC (38).

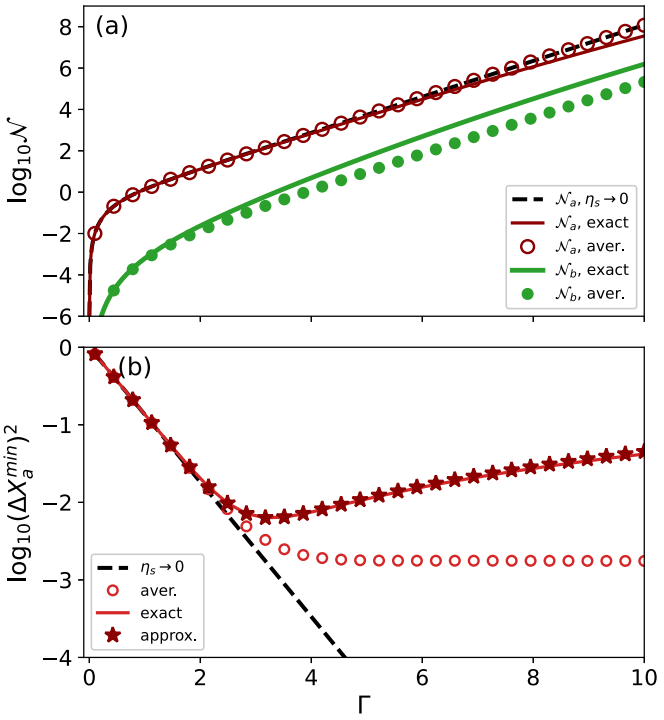

FIG. 5. (a) Number of photons for PDC and CUpC and (b) minimal quadrature variance for PDC mode as a function of parametric gain Γ. The calculation is obtained with $\Delta_s L = 15\pi$ and $r = |\eta_s|/|\kappa| = 1$ for different models: exact, averaged, and PDC with the absence of CUpC ($\eta_s \to 0$). The approximate expression (47) is in good agreement with the exact solution.

Otherwise, for the minimal quadrature variance, different models lead to different results. In the absence of CUpC, the minimal quadrature variance is decreasing with the pump power (39). The presence of non-phase-matched CUpC leads to the limitation of quadrature squeezing but the dependences calculated with exact and averaged models are completely different: The exact solution provides the local minimum, while the averaged solution results in plateau.

The difference between these two solutions is provided by different regimes of generation: The averaging procedure transfers the solution from area II into area IV that leads to different spatial dynamics of CUpC. In addition, the averaged solution is extremely sensitive to the value of $\Delta_s L$: The averaged coupling coefficient $|\zeta(\Delta)| \sim |\mathrm{sinc}(\Delta_s L/2)|$ [Eq. (19)] depends periodically on the argument and consequently reaches local maximum when $\Delta_s L = n\pi$ (n is odd). When $\Delta_s L = m\pi$ (m is even) the averaged coupling coefficient $\zeta(\Delta) = 0$ and the CUpC is absent, in opposite to the exact solution that always gives the nonzero CUpC and does not strongly depend on $\Delta_s L$.

A few words should be devoted to the necessity of taking into consideration CUpC when squeezed states via PDC are generated. One can notice that the maximal squeezing of the PDC mode is obtained when $\mathcal{N}_b \approx 1$ and the condition $\mathcal{N}_b < 1$ can be treated as the criterion when the CUpC can be neglected and optimal generation of single-mode squeezed PDC states can be achieved.

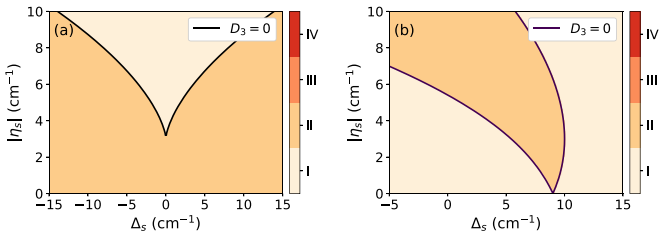

FIG. 6. Phase diagrams $\eta_s - \Delta_s$ for three-mode interaction for (a) phase-matched PDC $\widetilde{\Delta} = 0$ and (b) non-phase-matched PDC $\widetilde{\Delta} = 10$ cm^{-1}. Area I, oscillating solution for Bogoliubov functions; area II, parametric amplification exists.

IV. RESULTS AND DISCUSSION: NONDEGENERATE REGIME

In the previous section, the degenerate regime of PDC with CUpC is analyzed. In this section, we consider more complicated cases of nondegenerate regime of generation: three- and four-mode interaction.

A. Three-mode interaction

Let us consider the nondegenerate PDC generation when only one PDC mode (e.g., signal) is up-converted. This regime has been previously studied within simultaneous phase matching for PDC with CUpC [13,14,16]. It was shown that all three waves are parametric amplified if $|\kappa| > |\eta_s|$ and are oscillating if $|\kappa| < |\eta_s|$. Below, with the use of our approach, we extend this criterion on the non-phase-matched case.

So far as only signal PDC mode is up-converted, we set $\eta_i \to 0$ and $\Delta_i \to 0$. In this case, one of the roots of the initial quartic equation (21) is always imaginary $\lambda_4 = i\phi/2$ and the equation is reduced to the cubic one

$$\left[\lambda^2 - |\kappa|^2 + \frac{\phi^2}{4} + g_s^2\right]\left[\lambda + \frac{i\phi}{2}\right] - i\phi g_s^2 + \frac{i\Delta_s}{2}|\kappa|^2 = 0. \tag{49}$$

For the cubic polynomial, the discriminant has the form $D_3 = -4P_3^3 - 27Q_3^2$, where

$$P_3 = g_s^2 - |\kappa|^2 + \frac{\phi^2}{3}, \tag{50}$$

$$Q_3 = \frac{\Delta_s}{2}|\kappa|^2 - \frac{2\phi}{3}\left[g_s^2 + \frac{|\kappa|^2}{2} - \frac{\phi^2}{9}\right], \tag{51}$$

and $g_s^2 = |\eta_s|^2 + \Delta_s^2/4$, $\phi = \widetilde{\Delta} - \Delta_s/2$.

Thus, for the three-mode interaction, three regimes are realized:

(1) $D_3 < 0$, oscillating solution for Bogoliubov functions (all the roots are imaginary).

(2) $D_3 > 0$, parametric amplification (it should be noted that according the Vieta's formulas $\mathrm{Re}[\lambda_1 + \lambda_2 + \lambda_3] = 0$ and at least one of the root is always real and positive).

(3) $D_3 = 0$, multiple roots.

Figure 6(a) demonstrates the phase diagram $\eta_s - \Delta_s$ for the phase-matched PDC generation $\widetilde{\Delta} = 0$ cm^{-1} for $\kappa = 3$ cm^{-1}. The phase diagram $\eta_s - \Delta_s$ for the non-phase-matched PDC ($\widetilde{\Delta} = 10$ cm^{-1} and $\kappa = 3$ cm^{-1}) is shown in Fig. 6(b). One can see that the parametric amplification exists even if both the processes PDC and CUpC are non-phase-matched.

TABLE II. Conditions for different natures of roots of characteristic equation for the nondegenerate four-mode CUpC of PDC. $\mathbb{R}$ is real number, $\mathbb{I}$ is imaginary number, and $\mathbb{C}$ is complex with nonzero real and imaginary parts.

Area	Condition	Roots
I	$D > 0$ and $P > 0$ and $R < P^2/4$	$\lambda_{1,2,3,4} \in \mathbb{I}$
II	$D < 0$	$\lambda_{1,2} \in \mathbb{R}$, $\lambda_{3,4} \in \mathbb{I}$
III	($D > 0$ and $P > 0$ and $R > P^2/4$) or ($D > 0$, $P \leqslant 0$)	$\lambda_{1,2,3,4} \in \mathbb{C}$
V	$D = 0$	Multiple roots

B. Four-mode interaction: General analysis

Generally, the CUpC is present for both the signal and idler waves and all the parameters $\kappa, \eta_s, \eta_i, \widetilde{\Delta}, \Delta_s, \Delta_i$ are independent. According to Ref. [46], the nature of the roots of characteristic equation (21) is determined by the discriminant

$$D = 256R^3 - 128P^2R^2 + 144PQ^2R - 27Q^4 + 16P^4R - 4P^3Q^2, \tag{52}$$

and in Table II the different regimes are shown. In analogous way to the degenerate case (Subsec. III B) the parametric amplification is realized in the areas II and III, while the oscillating solution for the Bogoliubov functions exists in area I.

C. Four-mode interaction: Cascaded phase matching

In this subsections, we confine the discussion to some particular case of four-mode interaction, when the cascaded phase matching can be achieved. For PDC with CUpC, the cascaded wave-vector mismatches are introduced:

$$\Phi_s = \widetilde{\Delta} - \Delta_s = 2k_p - k_{ai} - k_{bs}, \tag{53}$$

$$\Phi_i = \widetilde{\Delta} - \Delta_i = 2k_p - k_{as} - k_{bi}, \tag{54}$$

$$\Phi_{si} = \widetilde{\Delta} - \Delta_s - \Delta_i = 3k_p - k_{bs} - k_{bi}. \tag{55}$$

It should be noted that cascaded phase matching can be realized when all the processes are simultaneously non-phase-matched: $\widetilde{\Delta} \neq 0$, $\Delta_s \neq 0$, and $\Delta_i \neq 0$.

Figure 7(a) shows the phase diagrams $\Delta_s - \Delta_i$ calculated for non-phase-matched PDC with $\widetilde{\Delta} = 30$ cm^{-1} and coupling parameters $\kappa = \eta_s = \eta_i = 3$ cm^{-1}. In spite of the fact that PDC is non-phase-matched, the parametric amplification exists (areas II and III) and the high-gain regime can be achieved. Strictly speaking, areas II and III are defined by the conditions from Table II; however, their location in the phase diagrams is close to the cascaded phase-matching conditions [Eqs. (55)]: Area II corresponds to the cascaded phase-matching conditions $\Phi_s \approx 0$ and $\Phi_i \approx 0$. In the phase diagram on the concurrence of lines $\Phi_s \approx 0$ and $\Phi_i \approx 0$, area III appears.

In Figs. 7(b)–7(d), the number of photons for different modes is present for high-gain regime. One can notice that in the case of $\Phi_i \approx 0$ [red dashed line in Fig. 7(a)] the

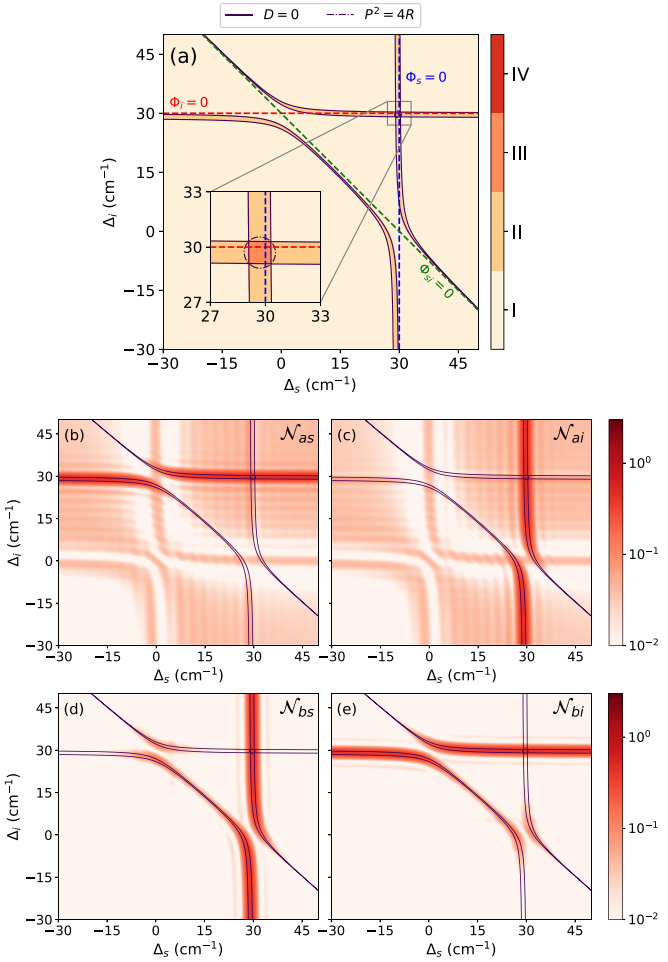

FIG. 7. Diagrams $\Delta_i - \Delta_s$ for four-mode CUpC with non-phase-matched PDC $\tilde{\Delta} = 0$. The coupling coefficients are $\kappa = \eta_s = \eta_i = 3\ \mathrm{cm}^{-1}$. (a) The phase diagram (different colors correspond to different areas from Table II). The dashed lines correspond to different cascaded phase matching. Panels (b), (c), (d), and (e) show the numbers of photons in PDC signal, PDC idler, CUpC signal, and CUpC idler modes, respectively, calculated for crystal length $L = 2$ cm.

amplification exists for signal PDC mode and idler CUpC mode $\mathcal{N}_{as} \approx \mathcal{N}_{bi}$ in Figs. 7(a) and 7(e). In the case of $\Phi_s \approx 0$ [blue dashed line in Fig. 7(a)], the situation is opposite: Amplification exists for idler PDC mode and signal CUpC mode [Figs. 7(c) and (d)]. In area III, near the intersection of red and blue dashed lines in Fig. 7(a), the intensities of all the modes are $\mathcal{N}_{as} \approx \mathcal{N}_{bs} \approx \mathcal{N}_{ai} \approx \mathcal{N}_{bi}$. For the cascaded phase-matching $\Phi_{si} = 0$, one can notice that the number of photons in CUpC modes is higher compared to the PDC ones.

Summing up, in this section the criteria for the parametric amplification in three- and four-mode generation are obtained. The parametric amplification takes place even if PDC and CUpC are separately non-phase-matched and the cascaded phase matching can be realized.

V. CONCLUSIONS

In summary, the exact solution in terms of Bogoliubov transformation for PDC with CUpC with nonzero wave-vector mismatches is presented. The simple relations, based on roots analysis of characteristic equation, for oscillating and parametric amplification regimes for CUpC of PDC are obtained for degenerate and three- and four-mode generation. We demonstrate that the high-gain regime of PDC with CUpC is determined not only by phase-matching conditions for each separate process, but also by the cascaded phase-matching conditions.

For the degenerate PDC generation, we show that the CUpC can be assumed as losses for the PDC radiation. The presence of CUpC leads to the limitation of minimal quadrature variance of PDC mode that can be crucial for practical generation of squeezed light via PDC.

So far as the solution is obtained in Heisenberg picture and has the form of Bogoliubov transformation, it is valid for any initial state of light. Here we confine ourself to the vacuum input state and present the analysis of a mean number of photons and minimal quadrature variance of interacting modes. However, from the general point of view, the studied system corresponds to the class of Gaussian unitaries [48] and all the methods for such systems can be applied for CUpC of PDC.

The results obtained in this paper can be used for the noise analysis in quantum frequency converters and for the development of new types of entangled and squeezed visible and UV light sources based on nonlinear crystals, periodically and aperiodically poled nonlinear crystals, and nonlinear waveguides.

ACKNOWLEDGMENTS

The authors thank T. V. Murzina for helpful discussions and supporting. D.A.K. acknowledges the financial support of RF President's Foundation for State Support of Young Russian Scientists (Grant No. MK-5886.2021.1.2). A.V.R acknowledges the financial support of Theoretical Physics and Mathematics Advancement Foundation BASIS (Grant No. 20-2-9-8-1).

APPENDIX A: BOGOLIUBOV TRANSFORMATION

In general, the Bogoliubov transformation can be written in the form [48]

$$\begin{bmatrix} \hat{\mathbf{b}} \\ \hat{\mathbf{b}}^\dagger \end{bmatrix} = \begin{bmatrix} \mathcal{A} & \mathcal{B} \\ \mathcal{B}^* & \mathcal{A}^* \end{bmatrix} \begin{bmatrix} \hat{\mathbf{a}} \\ \hat{\mathbf{a}}^\dagger \end{bmatrix} + \begin{bmatrix} d \\ d^\dagger \end{bmatrix}. \tag{A1}$$

For the system studied in this paper,

$$\begin{aligned} \hat{\mathbf{b}} &= [\hat{\alpha}_s(z), \hat{\alpha}_i(z), \hat{\beta}_s(z), \hat{\beta}_i(z)]^T, \\ \hat{\mathbf{b}}^\dagger &= [\hat{\alpha}_s^\dagger(z), \hat{\alpha}_i^\dagger(z), \hat{\beta}_s^\dagger(z), \hat{\beta}_i^\dagger(z)]^T, \\ \hat{\mathbf{a}} &= [\hat{\alpha}_s(0), \hat{\alpha}_i(0), \hat{\beta}_s(0), \hat{\beta}_i(0)]^T, \\ \hat{\mathbf{a}}^\dagger &= [\hat{\alpha}_s^\dagger(0), \hat{\alpha}_i^\dagger(0), \hat{\beta}_s^\dagger(0), \hat{\beta}_i^\dagger(0)]^T, \end{aligned} \tag{A2}$$

and $d = [0, 0, 0, 0]^T$, $d^\dagger = [0, 0, 0, 0]^T$.

According to the Heisenberg equation (15), the system is closed under operators $\hat{\alpha}_s(z)$, $\hat{\alpha}_i^\dagger(z)$, $\hat{\beta}_s(z)$, $\hat{\beta}_i^\dagger(z)$, and

consequently the matrices $\mathcal{A}$ and $\mathcal{B}$ have the form

$$\mathcal{A}=\begin{bmatrix} U_s(z) & 0 & W_s(z) & 0 \\ 0 & U_i(z) & 0 & W_i(z) \\ K_s(z) & 0 & M_s(z) & 0 \\ 0 & K_i(z) & 0 & M_i(z) \end{bmatrix}, \tag{A3}$$

$$\mathcal{B}=\begin{bmatrix} 0 & V_s(z) & 0 & Q_s(z) \\ V_i(z) & 0 & Q_i(z) & 0 \\ 0 & L_s(z) & 0 & N_s(z) \\ L_i(z) & 0 & N_i(z) & 0 \end{bmatrix}. \tag{A4}$$

So far as Bogoliubov transformation is canonical [operators $\hat{\alpha}_s(z), \hat{\alpha}_i(z), \hat{\beta}_s(z), \hat{\beta}_i(z)$ are bosonic with the commutation relations (2)], the following conditions should be satisfied for any z:

$$\mathcal{A}\mathcal{A}^\dagger - \mathcal{B}\mathcal{B}^\dagger = \mathbb{I}_4,\ \mathcal{A}\mathcal{B}^T = (\mathcal{A}\mathcal{B}^T)^T. \tag{A5}$$

This conditions can be explicitly written for Bogoliubov functions,

$$|U_s|^2 + |W_s|^2 - |V_s|^2 - |Q_s|^2 = 1, \tag{A6}$$

$$|K_s|^2 + |M_s|^2 - |L_s|^2 - |N_s|^2 = 1, \tag{A7}$$

$$U_s^* K_s + W_s^* M_s = V_s^* L_s + Q_s^* N_s, \tag{A8}$$

$$U_s V_i + W_s Q_i = U_i V_s + W_i Q_s, \tag{A9}$$

$$K_s L_i + M_s N_i = K_i L_s + M_i N_s, \tag{A10}$$

$$U_s L_i + W_s N_i = K_i V_s + M_i Q_s. \tag{A11}$$

These conditions are valid for replaced indexes $i \leftrightarrow s$.

APPENDIX B: ANALYTICAL SOLUTION OF DIFFERENTIAL SYSTEMS

Let us consider the differential system

$$\begin{cases} \frac{d}{dz}Y_1 = iae^{i\Delta_1 z}Y_2 + ib^* e^{i\Delta_2 z}Y_3, \\ \frac{d}{dz}Y_2 = -ia^* e^{-i\Delta_1 z}Y_1 - ice^{-i\Delta_3 z}Y_4, \\ \frac{d}{dz}Y_3 = ibe^{-i\Delta_2 z}Y_1, \\ \frac{d}{dz}Y_4 = -ic^* e^{i\Delta_3 z}Y_2. \end{cases} \tag{B1}$$

By excluding Y_3 and Y_4 and introducing the new functions $\bar{Y}_1 = Y_1 e^{-i\Delta_1 z/2 + i(\Delta_3-\Delta_2)z/4}$, $\bar{Y}_2 = Y_2 e^{i\Delta_1 z/2 + i(\Delta_3-\Delta_2)z/4}$, one can obtain the autonomous system

$$\begin{cases} \left[\left(\frac{d}{dz}+\frac{i\phi}{2}\right)^2 + g_b^2\right]\bar{Y}_1 = ia\left[\frac{d}{dz} + i\frac{\phi-\Delta_2}{2}\right]\bar{Y}_2, \\ \left[\left(\frac{d}{dz}-\frac{i\phi}{2}\right)^2 + g_c^2\right]\bar{Y}_2 = -ia^*\left[\frac{d}{dz} - i\frac{\phi-\Delta_3}{2}\right]\bar{Y}_1, \end{cases} \tag{B2}$$

where $g_b^2 = |b|^2 + \Delta_2^2/4$, $g_c^2 = |c|^2 + \Delta_3^2/4$, $\phi = \Delta_1 - (\Delta_2 + \Delta_3)/2$. Finally, we get a single differential equation of the fourth degree for the $\bar{Y}_1$:

$$\left[\frac{d^4}{dz^4} + P\frac{d^2}{dz^2} + iQ\frac{d}{dz} + R\right]\bar{Y}_1 = 0, \tag{B3}$$

where coefficients are given:

$$P = g_b^2 + g_c^2 + \frac{\phi^2}{2} - |a|^2, \tag{B4}$$

$$Q = \phi(g_c^2 - g_b^2) - |a|^2\frac{\Delta_3 - \Delta_2}{2}, \tag{B5}$$

$$R = \left[g_b^2 - \frac{\phi^2}{4}\right]\left[g_c^2 - \frac{\phi^2}{4}\right] - \frac{|a|^2}{4}(\phi - \Delta_3)(\phi - \Delta_2). \tag{B6}$$

The characteristic equation for this equation has the form

$$\lambda^4 + P\lambda^2 + iQ\lambda + R = 0. \tag{B7}$$

In the case of nonzero discriminant of Eq. (B7), it has distinct roots and the function Y_1 takes following form,

$$Y_1(z) = \sum_k \widetilde{C}_k e^{\alpha_k z}, \tag{B8}$$

where $\alpha_k \equiv \lambda_k + i(2\Delta_1 + \Delta_2 - \Delta_3)/4$ and coefficients $\widetilde{C}_k$ are determined by the initial conditions.

The functions $Y_2(z)$, $Y_3(z)$, and $Y_4(z)$ can be obtained from $Y_1(z)$ as

$$\begin{aligned} Y_3(z) &= ib\int_0^z dz'\, e^{-i\Delta_2 z'}Y_1(z'), \\ Y_2(z) &= \frac{e^{-i\Delta_1 z}}{ia}\frac{\partial Y_1(z)}{\partial z} - \frac{b^* e^{i(\Delta_2-\Delta_1)z}}{a}Y_3(z), \\ Y_4(z) &= -ic^*\int_0^z dz'\, e^{i\Delta_3 z'}Y_2(z'). \end{aligned} \tag{B9}$$

1. Analytical solution for Bogoliubov functions $U(z)$, $V(z)$, $K(z)$, $L(z)$

It can be noticed that differential system (17) for the functions $U(z)$, $V(z)$, $K(z)$, $L(z)$ has the form (B1) with the initial conditions $Y_1(z) = 1, Y_2(z) = 0, Y_3(z) = 0, Y_4(z) = 0$.

According to (B8), the function has the form

$$Y_1(z) = \sum_k C_k e^{\alpha_k z}, \tag{B10}$$

where $\alpha_k \equiv \lambda_k + i\Delta_1/2 - i(\Delta_3 - \Delta_2)/4$.

By substitution the solution (B10) into the initial conditions

$$\begin{aligned} Y_1(0) = 1,\ \frac{\partial Y_1}{\partial z}(0) = 0,\ \frac{\partial^2 Y_1}{\partial z^2}(0) = |a|^2 - |b|^2, \\ \frac{\partial^3 Y_1}{\partial z^3}(0) = i(\Delta_1|a|^2 - \Delta_2|b|^2), \end{aligned} \tag{B11}$$

the coefficients C_k are determined by the equation

$$\begin{pmatrix} 1 & 1 & 1 & 1 \\ \alpha_1 & \alpha_2 & \alpha_3 & \alpha_4 \\ \alpha_1^2 & \alpha_2^2 & \alpha_3^2 & \alpha_4^2 \\ \alpha_1^3 & \alpha_2^3 & \alpha_3^3 & \alpha_4^3 \end{pmatrix}\begin{pmatrix} C_1 \\ C_2 \\ C_3 \\ C_4 \end{pmatrix} = \begin{pmatrix} 1 \\ 0 \\ |a|^2 - |b|^2 \\ i(\Delta_1|a|^2 - \Delta_2|b|^2) \end{pmatrix}. \tag{B12}$$

The explicit form of the functions is

$$Y_2(z) = \frac{e^{i\delta_3 z}}{ia}\sum_{k=1}^{4} C_k[\alpha_k e^{\xi_1 z} + |b|^2 F(z,\xi_1)], \tag{B13}$$

$$Y_3(z) = ib\sum_{k=1}^{4} C_k F(z,\xi_1), \tag{B14}$$

$$Y_4(z) = -\frac{c^*}{a}\sum_{k=1}^{4} C_k\left[\left(\alpha_k + \frac{|b|^2}{\xi_1}\right)F(z,\xi_2) - \frac{|b|^2}{\xi_1}F(z,\delta_4)\right], \tag{B15}$$

where $F(z,\gamma) \equiv (e^{\gamma z}-1)/\gamma$, $\xi_1 = \alpha_k - i\Delta_2$, $\xi_2 = \alpha_k - i\Delta_1 + i\Delta_3$, $\delta_3 = \Delta_2 - \Delta_1$, and $\delta_4 = i\Delta_2 + i\Delta_3 - i\Delta_1$.

The Bogoliubov functions are determined in the following way: $U_s(z) = Y_1(z)$, $V_i^*(z) = Y_2(z)$, $K_s(z) = Y_3(z)$, $L_i^*(z) = Y_4(z)$, with the coefficients $a = \kappa$, $b = \eta_s$, $c = \eta_i$, $\Delta_1 = \Delta$, $\Delta_2 = \Delta_s$, $\Delta_3 = \Delta_i$.

The Bogoliubov functions for the replaced lower indexes are determined in the following way: $U_i(z) = Y_1(z)$, $V_s^*(z) = Y_2(z)$, $K_i(z) = Y_3(z)$, $L_s^*(z) = Y_4(z)$, with the coefficients $a = \kappa$, $b = \eta_i$, $c = \eta_s$, $\Delta_1 = \Delta$, $\Delta_2 = \Delta_i$, $\Delta_3 = \Delta_s$.

2. Analytical solution for Bogoliubov functions $W(z)$, $Q(z)$, $M(z)$, $N(z)$

In the same manner as in the previous subsection, the functions $W(z)$, $Q(z)$, $M(z)$, $N(z)$ can be found from the system (B1) with the initial conditions $Y_1(z) = 0$, $Y_2(z) = 0$, $Y_3(z) = 1$, $Y_4(z) = 0$.

In this case, the (B8) the solution has the form

$$Y_1(z) = \sum_k D_k e^{\alpha_k z}, \tag{B16}$$

where $\alpha_k \equiv \gamma_k + i\delta$. The coefficients D_k are determined by the equation

$$\begin{pmatrix} 1 & 1 & 1 & 1 \\ \alpha_1 & \alpha_2 & \alpha_3 & \alpha_4 \\ \alpha_1^2 & \alpha_2^2 & \alpha_3^2 & \alpha_4^2 \\ \alpha_1^3 & \alpha_2^3 & \alpha_3^3 & \alpha_4^3 \end{pmatrix}\begin{pmatrix} D_1 \\ D_2 \\ D_3 \\ D_4 \end{pmatrix} = \begin{pmatrix} 0 \\ ib^* \\ -b^*\Delta_2 \\ ib^*(|a|^2 - |b|^2 - \Delta_2^2) \end{pmatrix}, \tag{B17}$$

which is obtained in the same way as in the previous subsection.

The explicit form of the functions is

$$Y_2(z) = \frac{e^{i\delta_3 z}}{ia}\left(-ib^* + \sum_{k=1}^{4} D_k[\alpha_k e^{\xi_1 z} + |b|^2 F(z,\xi_1)]\right), \tag{B18}$$

$$Y_3(z) = 1 + ib\sum_{k=1}^{4} D_k F(z,\xi_1), \tag{B19}$$

$$Y_4(z) = -\frac{c^*}{a}\left[\sum_{k=1}^{4} D_k\left(\alpha_k + \frac{|b|^2}{\xi_1}\right)F(z,\xi_2) - \left(\sum_{k=1}^{4}\frac{|b|^2 D_k}{\xi_1} + ib^*\right)F(z,\delta_4)\right]. \tag{B20}$$

The Bogoliubov functions are determined in the following way: $W_s(z) = Y_1(z)$, $Q_i^*(z) = Y_2(z)$, $M_s(z) = Y_3(z)$, $N_i^*(z) = Y_4(z)$, with the coefficients $a = \kappa$, $b = \eta_s$, $c = \eta_i$, $\Delta_1 = \Delta$, $\Delta_2 = \Delta_s$, $\Delta_3 = \Delta_i$.

The Bogoliubov functions with the replaced lower indexes are $W_i(z) = Y_1(z)$, $Q_s^*(z) = Y_2(z)$, $M_i(z) = Y_3(z)$, $N_s^*(z) = Y_4(z)$, with the coefficients $a = \kappa$, $b = \eta_i$, $c = \eta_s$, $\Delta_1 = \Delta$, $\Delta_2 = \Delta_i$, $\Delta_3 = \Delta_s$.

3. Comments on characteristic equation

a. Interchange of idler and signal modes

It could seem that the systems (17) and (18) for replaced indexes $s \leftrightarrow i$ are determined by completely different characteristic equations. However, by applying this replacement for the characteristic equation (B7) ($b \leftrightarrow c$ and $\Delta_2 \leftrightarrow \Delta_3$), the second characteristic equation can be obtained:

$$\bar{\lambda}^4 + P\bar{\lambda}^2 - iQ\bar{\lambda} + R = 0. \tag{B21}$$

The roots $\bar{\lambda}_i$ and roots for (B7) λ_i are related as

$$\bar{\lambda}_i = \lambda_i^*. \tag{B22}$$

Consequently, any of characteristic equations (B7) or (B21) can be used for the parametric amplification analysis (see Subsec. II B).

b. Characteristic equation analysis with complex coefficients

The consideration of quartic polynomial is conventionally carried out for real coefficients [46]. In the characteristic equation (B7), the imaginary unit by the linear term λ is present. After the replacement $\mu = i\lambda$, the initial equation (B7) is reduced to the form with the real coefficients $\mu^4 - P\mu^2 + Q\mu + R = 0$. From this point, the roots analysis performed in Ref. [46] can be exploited.

[1] D. Klyshko, *Photons and Nonlinear Optics* (CRC Press, Boca Raton, FL, 1988).

[2] B. Brecht, D. V. Reddy, C. Silberhorn, and M. G. Raymer, Phys. Rev. X **5**, 041017 (2015).

[3] C. Fabre and N. Treps, Rev. Mod. Phys. **92**, 035005 (2020).

[4] D. F. Walls, Nature (London) **306**, 141 (1983).

[5] M. Chekhova, G. Leuchs, and M. Żukowski, Opt. Commun. **337**, 27 (2015).

[6] Y. Shih, Rep. Prog. Phys. **66**, 1009 (2003).

[7] J. Aasi, J. Abadie, B. P. Abbott, R. Abbott, T. D. Abbott, M. R. Abernathy, C. Adams, T. Adams, P. Addesso, R. X. Adhikari *et al.*, Nat. Photon. **7**, 613 (2013).

[8] H. Vahlbruch, M. Mehmet, K. Danzmann, and R. Schnabel, Phys. Rev. Lett. **117**, 110801 (2016).

[9] S. M. Saltiel, A. A. Sukhorukov, and Y. S. Kivshar, Prog. Opt. **47**, 1 (2005).

[10] S. Akhmanov and R. V. Khokhlov, *Problems of Nonlinear Optics: Electromagnetic Waves in Nonlinear Dispersive Media* (Gordon and Breach, New York, 1972), p. 294.

[11] R. A. Andrews, H. Rabin, and C. L. Tang, Phys. Rev. Lett. **25**, 605 (1970).

[12] S. Arakelyan, V. Tunkin, A. Kholodny, and A. Chirkin, J. Tech. Phys. **44**, 1253 (1974).

[13] C. L. Tang, Phys. Rev. **182**, 367 (1969).

[14] E. A. Mishkin and D. F. Walls, Phys. Rev. **185**, 1618 (1969).

[15] D. Klyshko and N. Nazarova, Zh. Eksp. Teor. Fiz. **58**, 878 (1970) [Sov. Phys.-JETP **31**, 472 (1970)].

[16] M. E. Smithers and E. Y. C. Lu, Phys. Rev. A **10**, 1874 (1974).

[17] Y. A. Ilinskii, D. N. Klyshko, and V. M. Petnikova, Sov. J. Quantum Electron. **5**, 1343 (1975).

[18] A. Ferraro, M. G. A. Paris, M. Bondani, A. Allevi, E. Puddu, and A. Andreoni, J. Opt. Soc. Am. B **21**, 1241 (2004).

[19] E. Puddu, A. Allevi, A. Andreoni, and M. Bondani, J. Opt. Soc. Am. B **21**, 1839 (2004).

[20] A. Allevi, M. Bondani, A. Ferraro, and M. G. A. Paris, Laser Phys. **16**, 1451 (2006).

[21] A. Allevi, M. Bondani, M. G. A. Paris, and A. Andreoni, Phys. Rev. A **78**, 063801 (2008).

[22] J. Sun, S. Zhang, T. Jia, Z. Wang, and Z. Sun, J. Opt. Soc. Am. B **26**, 549 (2009).

[23] J. Flórez, J. S. Lundeen, and M. V. Chekhova, Opt. Lett. **45**, 4264 (2020).

[24] J. Perina and J. Perina, Quant. Semiclass. Opt.: Eur. Opt. Soc. B **7**, 541 (1995).

[25] A. S. Chirkin, Quant. Semiclass. **4**, S91 (2002).

[26] T. V. Tlyachev, A. M. Chebotarev, and A. S. Chirkin, Phys. Scr. **T160**, 014041 (2014).

[27] I. I. Arkhipov, J. Perina, O. Haderka, A. Allevi, and M. Bondani, Sci. Rep. **6**, 33802 (2016).

[28] M. Mancinelli, A. Trenti, S. Piccione, G. Fontana, J. S. Dam, P. Tidemand-Lichtenberg, C. Pedersen, and L. Pavesi, Nat. Commun. **8**, 15184 (2017).

[29] A. Barh, P. J. Rodrigo, L. Meng, C. Pedersen, and P. Tidemand-Lichtenberg, Adv. Opt. Photon. **11**, 952 (2019).

[30] V. Krutyanskiy, M. Meraner, J. Schupp, V. Krcmarsky, H. Hainzer, and B. P. Lanyon, npj Quantum Inf. **5**, 72 (2019).

[31] J. S. Pelc, C. Langrock, Q. Zhang, and M. M. Fejer, Opt. Lett. **35**, 2804 (2010).

[32] H. Rutz, K.-H. Luo, H. Suche, and C. Silberhorn, Phys. Rev. Appl. **7**, 024021 (2017).

[33] N. Maring, D. Lago-Rivera, A. Lenhard, G. Heinze, and H. de Riedmatten, Optica **5**, 507 (2018).

[34] P. C. Strassmann, A. Martin, N. Gisin, and M. Afzelius, Opt. Expr. **27**, 14298 (2019).

[35] T. V. Tlyachev, A. M. Chebotarev, and A. S. Chirkin, Phys. Scr. **T153**, 014060 (2013).

[36] A. Christ, B. Brecht, W. Mauerer, and C. Silberhorn, New J. Phys. **15**, 053038 (2013).

[37] P. R. Sharapova, G. Frascella, M. Riabinin, A. M. Pérez, O. V. Tikhonova, S. Lemieux, R. W. Boyd, G. Leuchs, and M. V. Chekhova, Phys. Rev. Research **2**, 013371 (2020).

[38] Y. R. Shen, Phys. Rev. **155**, 921 (1967).

[39] B. Huttner, S. Serulnik, and Y. Ben-Aryeh, Phys. Rev. A **42**, 5594 (1990).

[40] J. Perina, Phys. Rev. A **92**, 013833 (2015).

[41] T. Lipfert, D. B. Horoshko, G. Patera, and M. I. Kolobov, Phys. Rev. A **98**, 013815 (2018).

[42] D. B. Horoshko, L. LaVolpe, F. Arzani, N. Treps, C. Fabre, and M. I. Kolobov, Phys. Rev. A **100**, 013837 (2019).

[43] B. Dayan, Phys. Rev. A **76**, 043813 (2007).

[44] D. A. Kopylov, A. V. Rasputnyi, T. V. Murzina, and M. V. Chekhova, Laser Phys. Lett. **17**, 075401 (2020).

[45] K. Thapliyal, A. Pathak, B. Sen, and J. Perina, Phys. Rev. A **90**, 013808 (2014).

[46] E. L. Rees, Am. Math. Mon. **29**, 51 (1922).

[47] L. Caspani, E. Brambilla, and A. Gatti, Phys. Rev. A **81**, 033808 (2010).

[48] C. Weedbrook, S. Pirandola, R. Garcia-Patron, N. J. Cerf, T. C. Ralph, J. H. Shapiro, and S. Lloyd, Rev. Mod. Phys. **84**, 621 (2012).